CISTER
Research Center in
Real-Time & Embedded
Computing Systems

Technical Report

Mobile IoT: smart-HOP over RPL

Hossein Fotouhi
Daniel Moreira
Mário Alves

CISTER-TR-140709
Version:
Date:

Mobile IoT: smart-HOP over RPL

Hossein Fotouhi, Daniel Moreira, Mário Alves

CISTER Research Unit

Polytechnic Institute of Porto (ISEP-IPP)

Rua Dr. António Bernardino de Almeida, 431

4200-072 Porto

Portugal

Tel.: +351.22.8340509, Fax: +351.22.8340509

E-mail:

http://www.cister.isep.ipp.pt

Abstract

The 6loWPAN (the light version of IPv6) and RPL (routing protocol for low-power and lossy links) protocols have become de facto standards for the Internet of Things (IoT). In this paper, we show that the two native algorithms that handle changes in network topology --the Trickle and Neighbor Discovery algorithms-- behave in a reactive fashion and thus are not prepared for the dynamics inherent to nodes' mobility. Many emerging and upcoming IoT application scenarios are expected to impose real-time and reliable mobile data collection, which is not compatible with the long message latency and high packet loss exhibited by the native RPL/6loWPAN protocols. To solve this problem, we integrate a proactive hand-off mechanism (dubbed smart-HOP) within RPL, which is very simple, effective and backward compatible with the standard protocol. We show that this add-on halves the packet loss and reduces the hand-off delay dramatically to one tenth of a second, upon nodes' mobility, with a sub-percent overhead. The smart-HOP algorithm has been implemented and integrated in the Contiki 6LoWPAN/RPL stack (source-code available online) and validated through extensive simulation and experimentation.

Mobile IoT: smart-HOP over RPL

Hossein Fotouhi, Daniel Moreira and Mário Alves[1]
Polytechnic Institute of Porto, CISTER/INESC-TEC, ISEP

Abstract

The 6loWPAN (the light version of IPv6) and RPL (routing protocol for low-power and lossy links) protocols have become *de facto* standards for the Internet of Things (IoT). In this paper, we show that the two native algorithms that handle changes in network topology —the Trickle and Neighbor Discovery algorithms— behave in a reactive fashion and thus are not prepared for the dynamics inherent to nodes' mobility. Many emerging and upcoming IoT application scenarios are expected to impose real-time and reliable mobile data collection, which is not compatible with the long message latency and high packet loss exhibited by the native RPL/6loWPAN protocols. To solve this problem, we integrate a proactive hand-off mechanism (dubbed smart-HOP) within RPL, which is very simple, effective and backward compatible with the standard protocol. We show that this add-on halves the packet loss and reduces the hand-off delay dramatically to one tenth of a second, upon nodes' mobility, with a sub-percent overhead. The smart-HOP algorithm has been implemented and integrated in the Contiki 6LoWPAN/RPL stack (source-code available online [1]) and validated through extensive simulation and experimentation.

Keywords: `Wireless Sensor Networks, Internet of Things, Mobility, RPL, hand-off, Test-bed.`

Email address: `(mohfg,dadrm,mjf)@isep.ipp.pt` (Hossein Fotouhi, Daniel Moreira and Mário Alves)

1. Introduction

The next generation Internet, commonly referred as *Internet of Things* (IoT), depicts a world populated by an endless number of smart devices that are able to sense, process, react to the environment, cooperate and intercommunicate via the Internet. For over a decade, low-power wireless network research contested the complexity of the Internet architecture for sensor network applications. However, as the state-of-the-art progressed, academic and commercial efforts invented new network abstractions based on the Internet architecture. The *Internet Engineering Task Force* (IETF) designed some protocols and adaptation layers that allow IPv6 to run over the IEEE 802.15.4 link layer. The *IPv6 over Low-power Wireless Personal Area Networks* (6LoWPAN) working group [2] designed header compression and fragmentation for IPv6 over IEEE 802.15.4 [3]. The IETF *Routing Over Low-power and Lossy networks* (ROLL) working group designed a routing protocol, referred as RPL [4], which is the *de-facto* standard routing protocol for 6LoWPAN. These standard IP-based protocols are thus a fundamental building block for the IoT.

Mobility support is becoming a requirement in various emerging IoT applications [5, 6, 7], including health-care monitoring, industrial automation and smart grids [8, 9, 10]. Many recent research projects and studies have considered the cooperation between mobile and fixed sensor nodes [11, 12, 13, 14]. In clinical monitoring [15], patients have embedded wireless sensing devices that report data in real-time. In oil refineries, the vital signs of workers are collected continuously in order to monitor their health situation in dangerous environments [16]. In fact, many applications require timeliness and reliability guarantees for transmitting critical messages from source to destination, but providing *Quality of Service* (QoS) in low-power and mobile networks is very challenging.

In this work, we are considering a wireless clinical monitoring application that collects patients' vital signs. Patients are mobile nodes that generate traffic and freely move while maintaining their connectivity with the fixed nodes

infrastructure. All nodes in our system model are simple sensor nodes featuring low-power CC2420 radio. Figure 1 illustrates the system model, where a MN moves from the vicinity of Node 8 toward Node 7. We propose a hand-off mechanism that quickly detects mobile entities and locally updates the routing tree. *Hand-off is referred as the process of switching a MN from one point of attachment to another.* In this process, the standard RPL routing performs normally while the mobile nodes run a hand-off algorithm. We build on smart-HOP, which is a hard hand-off mechanism that was designed and tested in a generic network architecture, in a protocol-agnostic way [17, 18].

Two main mechanisms are employed in RPL and 6LoWPAN that partially cope with mobility. First, the periodic transmission of control packets, scheduled by the *Trickle* algorithm, can detect topological changes. During this process, RPL resumes a fast global routing update that causes a high overhead. Second, the *Neighbor Discovery* (ND —defined in RFC 4861) mechanism, assesses the neighbor reachability in a regular basis. At each activation, the ND protocol floods the entire network with router advertisements, also leading to a high overhead. A short activation interval (that reduces the overhead) leads to low responsiveness to network/topological changes. However, in the revised ND mechanism of 6LoWPAN, router advertisement packets are transmitted upon receiving router solicitation messages [19].

Why smart-HOP? Hand-off has been widely studied in Cellular and wireless local area networks [20, 21, 22, 23]. However, it has not received the same level of attention in low-power networks. Cellular networks perform centralized hand-off decisions typically coordinated by powerful base-stations. Contrarily to Cellular networks, WiFi networks have a distributed architecture where hand-off is triggered when the quality of the service degrades. In low-power networks, a centralized approach is not feasible as the access points are assumed to have scarce resources. smart-HOP [17, 18] considers the main features of low-power networks, the link unreliability and the existence of a single low-power radio per node. It manages hand-offs in a distributed way and leads to very short disconnection times.

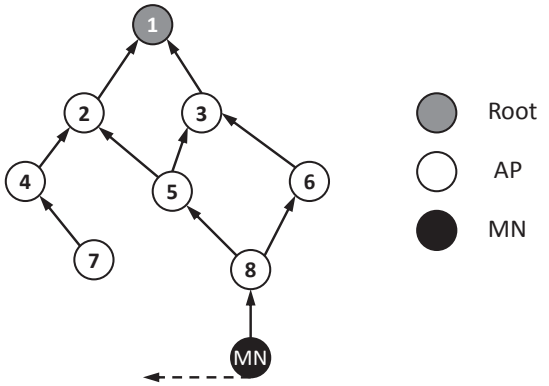

Figure 1: An example of having mobile node within an RPL tree, where the MN moves from the vicinity of AP_8 toward AP_7.

Why integrating smart-HOP in RPL? There are four main RPL features that motivated us to grant it with mobility support: (i) the proactive feature of RPL that generates and maintains stable routing tables. A periodic broadcast of control messages among all nodes maintains the paths and link states between them. In reactive routing protocols; such as AODV [24] and DSR [25], routes are established upon request, so they do not respond quickly to environmental changes due to mobility or link degradation. RPL maintains the route in the background with minimal overhead. Moreover, for an application with limited mobility and the requirement of an infrastructure, RPL is very suitable, (ii) unlike other proactive routing protocols (e.g. OSPF [26]), RPL exchanges local information among neighbors to repair routing inconsistencies, instead of globally advertising control messages, (iii) RPL runs a tree-based structure that is suitable for data collection WSN applications, and (iv) the IPv6-based addressing in RPL naturally performs the interoperability with other Internet devices.

Contributions. Building on our previous works [17, 18], we provide fast and reliable mobility support in RPL. The proposed mobility solution keeps the standard RPL protocol unchanged while providing backward compatibility with the standard implementation, i.e. standard and smart-HOP-enabled nodes can coexist and inter-operate in the same network. The main contributions of this

paper are:

1. efficient hand-off mechanism for RPL with good performance, correctly delivering nearly 100% packets with at most 90 ms hand-off delay and $< 1\%$ additional overhead upon nodes' mobility;

2. smooth integration and backward compatibility with the standard RPL/6LoWPAN;

3. collision avoidance mechanism (to avoid collision during the hand-off process while collecting packets from neighbor APs) and loop avoidance mechanism (to avoid closed loops in RPL routing upon mobility);

4. simulation (Cooja) analysis and experimental validation with commodity hardware platforms in a reliable environment;

5. implementation over a SOTA operating system (Contiki), for which the open source is freely available [1].

Organization. We categorize the related works on mobility support in IP-based low-power networks in Section 2. Section 3 explains the basics of RPL: the control messages, objective function and the process to maintain routes upon link dynamics. A brief background on the smart-HOP hand-off mechanism is presented in Section 4. Then, a general picture of the mRPL design is described in Section 5, which is further detailed in Section 6[1]. The simulation and experimental set-ups, followed by the results and discussion are presented in Sections 7 and 8 respectively. Finally, we conclude the paper and outline the most relevant findings in Section 9.

2. Related works

The mobility support at the network layer of IP-based low-power networks is addressed within two main routing schemes of (i) mesh-under and (ii) route-over,

[1]In the remainder of the paper, the terms "RPL", "standard RPL" and "default RPL" are used interchangeably. The same applies to the "mRPL", "smart-HOP-enabled RPL" and "mobility-enabled RPL" terms.

based on the routing decision being taken at the adaptation layer or network layer, respectively [27, 28]. The mesh-under routing supports communication in a single broadcast domain, where all nodes can reach each other by sending a single IP datagram. This scheme within 6LoWPAN requires link-layer routing, since the multi-hop topology is abstracted by employing IPv6 support. The route-over routing supports a multi-hop mesh communication, where only immediate neighbors are reachable within a single link transmission. This scheme has been specified in RPL that enables network layer according to the IP architecture.

In the following subsections, we address some of the related works on mobility support that focus on the mesh-routing and route-over schemes. We summarize these works and their main features in Table 1, including the solution we propose in this paper —mRPL— for the readers' convenience.

2.1. Mobility solutions within 6LoWPAN

In [29, 30] a light version of Mobile IPv6 over 6LoWPAN is evaluated. In Mobile IPv6, movement detection is based on neighbor discovery, which is optional in 6LoWPAN [31]. In this work, authors proposed Mobinet that relies on overhearing in the neighborhood of a mobile node. By detecting any changes in the neighborhood, the mobile node sends router solicitation in order to resume the neighbor discovery. The overhearing requires receiving all unnecessary packets by neighbor APs, which increases the network overhead and consequently the energy consumption.

In LowMOB [32], the mobility detection is based on frequent beacon transmissions from the static nodes. A mobile node joins the AP with the highest RSSI level. The mobility support is based on conventional mobile IPv6. It also considers duty cycled APs, where the radios are turned off intermittently. By observing a low link quality at the current AP, it activates the next appropriate AP. To do so, the current AP performs a localization mechanism by using additional nodes, called mobility support points (MSPs), to find the direction of the MN. The conventional MIPv6 and the localization require many packet

exchanges and impractical in low-power networks.

The network of proxies (NoP) [16] provides a mobility support without interfering with the normal WSN behavior. Authors employ additional devices, which are called proxies. NoP devices are resource-unconstrained and handle the hand-off procedure (on behalf of sensor nodes). Proxies are responsible for monitoring the RSSI from MNs and share this information with other proxies. By analyzing this information, proxies decide for the next best parent of the MN.

2.2. Mobility solutions within RPL

In [33, 34], authors focus on mobility support in RPL. The system model assumes existence of a fixed set of nodes, while MNs get access to the fixed nodes directly or via multiple hops through other MNs. The mobility detection is obtained by employing a fixed timer (instead of the Trickle timer). The authors concluded that with higher DIO transmission, the connectivity increases, at the expense of additional overhead. Upon finding a new neighbor, immediate probing updates the ETX value to select the preferred parent in a timely fashion. To avoid loops after hand-off, the child nodes are discarded from the parent set. The proposed model has high overhead in terms of fixed and periodic beaconing. Moreover, it disables the Trickle timer, which is very useful in the absence of mobility.

ME-RPL [35] assumes that mobile nodes are identified within static RPL nodes. By enabling a learning algorithm, nodes that change their parent more often query their neighbors with lower DIS intervals. It means that the DIS interval is dynamic according to the network inconsistencies. The MNs select static nodes with high quality links as their best parents. In this model, sudden movements are not detected in real-time, since a learning algorithm is used. Thus, the problem of low responsiveness of the RPL routing to detect environmental changes and inconsistencies still exists.

MoMoRo [36] supports mobility in a sparse traffic network that running RPL. It creates an additional layer between the data link and network layers to

Table 1: Mobility solutions in IP-based low-power networks

Reference	Routing mechanism	Mobility detection	Mobility solution	Additional hardware	Performance
[29, 30]	mesh-under	overhearing	light MIPv6	no	high overhead high energy high responsive
LowMOB [32]	mesh-under	periodic beaconing	MIPv6	yes	high overhead high energy moderate responsive
NoP [16]	mesh-under	periodic beaconing	MIPv6	yes	high overhead high energy high responsive
[33, 34]	route-over	fixed DIO	immediate ETX update	no	high overhead high energy high responsive
ME-RPL [35]	route-over	Trickle	adaptive DIS	no	low overhead low energy low responsive
MoMoRo [36]	route-over	packet loss	immediate beaconing	no	low overhead low energy low responsive
mRPL	route-over	Timers + Trickle + data packets	immediate beaconing	no	low overhead low energy high responsive

handle mobility detection. After a packet transmission failure, MoMoRo makes one more attempt to reach the destination by transmitting a unicast packet. If it fails again, MoMoRo starts searching for a new route by broadcasting beacons and collecting replies from neighbors. In this model, mobility detection depends only on the packet loss. This passive approach makes the network very low responsive to topological changes caused by mobility. Moreover, in low-power networks, it is very usual for the links quality to drop temporarily, causing packet loss, so a hand-off decision based on packet losses imposes unnecessary route maintenance that consequently increases network overhead.

3. Relevant aspects of the RPL protocol

RPL is an IPv6 distance vector routing protocol that operates on top of the IEEE 802.15.4 Physical and Data Link Layers and is appropriate for low-power wireless networks with very limited energy and bandwidth resources. The data rate is typically low (less than 250 kbps) and the communication is prone to high error rates, resulting in low data throughput.

RPL organizes node in a *Destination Oriented Directed Acyclic Graph* (DODAG), depicted in Figure 1. Each RPL router identifies a set of stable parents, each of which is a potential next hop on a path toward the "root" of the DODAG. A parent with the best link quality to the root is selected as the "preferred parent". A network may encompass several DODAGs, which are identified by the following parameters:

1. *RPLInstanceID*. This is used to identify an independent set of DODAGs that is optimized for a given scenario.

2. *DODAGID*. This is an identifier of a DODAG root. The *DODAGID* is unique within the scope of an *RPLInstanceID*.

3. *DODAGVersionNumber*. This parameter increments upon some specific events, such as rebuilding of a DODAG.

4. *Rank*. This parameter defines the node position with respect to the root node in a DODAG.

Each node in a DODAG is assigned a *rank* that increases in the downstream direction of the DAG and decreases in the upstream direction. For example, in Figure 1, Node 8 has higher rank than Node 5, and Node 5 has higher rank than Node 3 and Node 2.

RPL control messages. The RPL control messages are the new type of *Internet Control Message Protocol version 6* (ICMPv6) — defined in RFC 2463. The RPL specification defines four types of control messages: (i) *DODAG Information Object* (DIO). The transmission of this message is issued by the root

node and then multicast by other nodes. This message holds the main information for constructing and maintaining a tree, e.g. current rank of a node, RPL Instance and root address, (ii) *DODAG Information Solicitation* (DIS). A node that requires a DIO message from neighbors, requests it by multicasting DIS message, (iii) *Destination Advertisement Object* (DAO). Each node propagates a DAO message upward (along the DODAG). Thus, this message enables the downward traffic from the root through the DODAG to this node, and (iv) *Destination Advertisement Object Acknowledgment (DAO-ACK)*. This unicast message is sent by a DAO recipient to acknowledge its successful reception.

Mobility detection in RPL. Mobility is indicated as one of the main sources of inconsistency in RPL [37]. Generally, there are two main approaches that help in detecting mobility; (i) the ICMPv6 packet transmission, controlled by the Trickle algorithm and (ii) the ICMPv6 packet transmission, controlled by the ND protocol, which are described below.

(i) RPL Trickle Algorithm. The traditional collection protocols in low-power networks typically broadcast control messages at a fixed time interval [38]. A small interval requires more bandwidth and energy. A large interval uses less bandwidth and energy but topological problems may occur due to the incapability to cope with the network dynamics. The basic idea of the Trickle algorithm (defined in RFC 6206) is to propagate beacons if there is a change in routing information.

RPL reduces the cost of propagating routing states by using a Trickle-based timer [39]. Trickle is an adaptive beaconing strategy aiming at fast recovery and low overhead. While the DIS packets are sent periodically from the routers until the first parent node is selected, a Trickle timer is used to schedule the transmission of DIOs. This timer allows the DIO intervals to exponentially increase when the network conditions are stable and quickly decrease to the minimum when noticeable changes in the network conditions are detected. The periodic Trickle timer t is bounded by the interval $[I_{min}, I_{max}]$, where I_{min} is the minimum interval defined in milliseconds by a base-2 value (e.g. $2^{12} = 4096$ ms), and $I_{max} = I_{min} \times 2^{I_{doubling}}$ is used to limit the number of times the I_{min} can

double. Assuming $I_{doubling} = 4$, the maximum interval is simply calculated as $I_{max} = 4096 \times 2^4 = 65536$ ms.

The Trickle algorithm is able to maintain the topology update globally in a short period of time. A node that detects an inconsistency in a DIO message (e.g. imposed by node mobility), sets t to I_{min} and updates the tree. If the DODAG remains consistent, t is doubled each time a DIO transmission occurs until it reaches I_{max}, keeping that value constant. When the network is stable, the Trickle timer gradually converges to its maximum interval. Upon mobility, this large interval results in a very low network responsiveness. After detecting any inconsistency in the network, the DIO period of all nodes in the network exponentially decreases, affecting network overhead.

(ii) IPv6 neighbor discovery approach. RPL may use the IPv6 neighbor discovery approach [31] for detecting environmental changes. The low-power links exploit an optimized version of ND, which has been developed by the IETF as an adaptation of neighbor discovery for 6LoWPAN [19]. The ND protocol allows nodes to detect neighbor unreachability and to discover new neighbors. This protocol is supported by four ICMPv6 control messages: (i) *Neighbor Solicitation* (NS): determines the link layer address of a neighbor and verifies if a neighbor is still reachable, (ii) *Neighbor Advertisement* (NA): this is the reply to a NS message and it is also sent periodically to announce link changes, (iii) *Router Solicitation* (RS): a request from the host node (mobile node in our system model) to its router asking for generating information, and (iv) *Router Advertisement* (RA): message sent by a router periodically or as a response to a RS message to advertise its (the router's) presence with the information of the link and the Internet parameters. The periodicity of these messages is usually very low, which reduces the responsiveness of the protocol. Increasing the intervals will significantly increase network overhead.

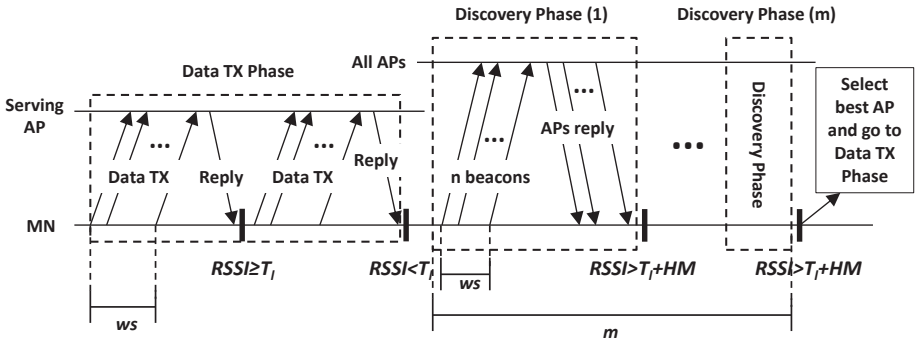

Figure 2: Timing diagram of the smart-HOP mechanism.

4. Background on smart-HOP

In this section, we provide a brief description on the design of smart-HOP and the main hand-off parameters involved. The smart-HOP algorithm has two main phases: (i) *Data Transmission Phase* and (ii) *Discovery Phase*. A timeline of the algorithm is depicted in Figure 2. For the sake of clarity, let us assume that a node is in the *Data Transmission Phase*. In this phase, the mobile node (MN) is assumed to have a reliable link with an access point (AP), defined as *Serving AP* in Figure 2. The mobile node monitors the link quality by receiving *reply* packets from the serving AP. Upon receiving n data packets in a given window, the serving AP replies with the average RSSI (ARSSI) or SNR of the n packets. If no packets are received, the AP takes no action. This may lead to disconnections, which are solved through the use of a time-out mechanism. It is important to notice that smart-HOP filters out asymmetric links implicitly by using reply packets at the Data Transmission and Discovery Phases. If a neighboring AP has no active links, that AP is simply not part of the process.

Hand-off parameters. The smart-HOP mechanism encompasses three main parameters [2] for fine-tuning:

Parameter 1: *window size (ws). ws* is the number of packets required to

[2]We ignored the stability monitoring parameter at this stage, since it has no impact on the smart-HOP performance [17]. The stability monitoring is the number of times in sequence that the MN detects a high quality link from an AP, in the *Discovery Phase*.

calculate the ARSSI over a specific time interval, as illustrated in Figure 2. A small ws provides detailed information about the link but increases the processing of reply packets, which leads to higher energy consumption and lower delivery rates. The packet delivery reduces as the MN opts for performing some unnecessary hand-offs. The hand-off is triggered by detecting low quality links, resulting from the decrease of the signal strength. On the other hand, a large ws provides only coarse grained information about the link and decreases the responsiveness of the system, which is not suitable for mobile networks with dynamic link changes.

Parameter 2: *hysteresis margin (HM).* This parameter is defined as the difference between the ARSSI threshold for starting the hand-off (T_l) and the ARSSI threshold for stopping the hand-off ($T_h \stackrel{\text{def}}{=} T_l + HM$). In WSNs, the selection of thresholds and *hysteresis margin*s is dictated by the characteristics of the transitional region and the variability of the wireless link. The thresholds should be selected according to the boundaries of the transitional region. The transitional region is often quite significant in size and hence a large number of links in the network (higher than 50%) are unreliable [40, 41]. Therefore, wireless nodes are likely to spend most of the time in the transitional region.

If the T_l threshold is too high, the node could perform unnecessary hand-offs (by being too selective). If the threshold is too low, the node may use unreliable links. The *hysteresis margin* plays a central role in coping with the variability of low-power wireless links. If the *hysteresis margin* is too narrow, the mobile node may end up performing unnecessary and frequent hand-offs between two APs (ping-pong effect). If the *hysteresis margin* is too large, hand-offs may take too long, which ends up increasing the network inaccessibility times, and thus decreasing the delivery rate.

Parameter 3: *stability monitoring (m).* Due to the high variability of wireless links, the mobile node may detect an AP that is momentarily above T_h, but the ARSSI may decrease shortly after handing-off to that AP. In order to avoid this, it is important to assess the stability of the candidate AP. After detecting an AP with the RSSI above T_h, the MN continues mm further Dis-

covery Phases to check the stability of that AP. As can be easily inferred, the *stability monitoring* and the *hysteresis margin* parameters are tightly coupled. A wide *hysteresis margin* requires a lower m, and vice-versa. [18] shows that an appropriate tuning of the *hysteresis margin* will lead to $m = 1$, which leads to a minimal overhead.

5. mRPL Overview

As previously mentioned, we are integrating smart-HOP within RPL in a way that is very simple, effective and backward compatible with the standard protocol. In this model, the standard RPL protocol is unchanged while providing mobility support, i.e. standard and smart-HOP enabled nodes can coexist and inter-operate in the same network.

The general procedure of beacon and data exchanges in smart-HOP integrated in RPL (mRPL) is similar to the original smart-HOP design, except employing RPL control messages (DIS and DIO) as beacons and adding some timers to improve reliability and efficiency. The timeline of algorithm is depicted in Figure 3. In this approach, the MN gets a reply packet (unicast DIO message) immediately after transmitting a predefined number of data packets (window size). The DIO reply message (that holds the average RSSI level), implicitly filters out the asymmetric links.

Upon detecting a good quality link (from the average RSSI level in the DIO reply message), the MN continues the *Data Transmission Phase*. By observing a ARSSI degradation, the MN starts in the *Discovery Phase*. However, the MN resumes the data communication with the serving AP until finding a better AP. After a successful hand-off, the nullifying process of the RPL algorithm is executed[3].

To assess the potential parents, the MN broadcasts a burst of DIS control messages. Then all neighbor APs reply to the MN in a non-conflicting basis

[3]Parent nullifying is a process in which the preferred parent is removed and the *rank* is set to infinity.

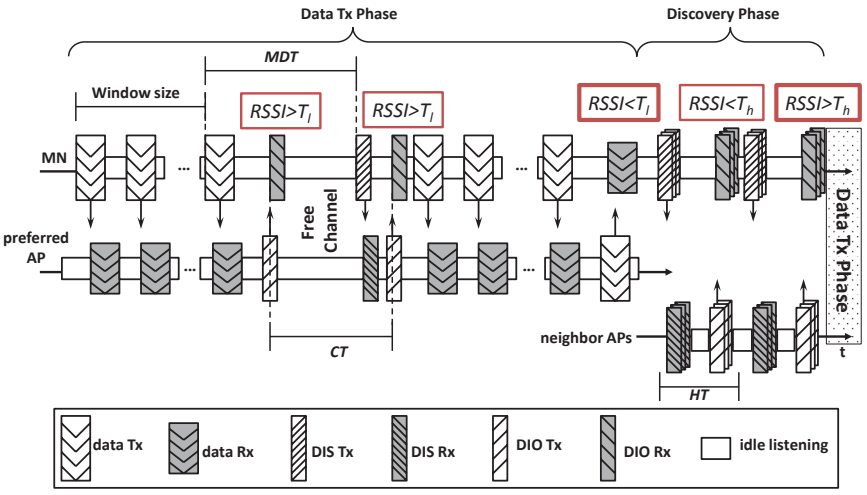

Figure 3: mRPL timing diagram for the *Data Tx Phase* and *Discovery Phase*.

(this will be discussed in detail later in this section). The average RSSI level is embedded in the unicast DIO reply. For each DIO reply received, the MN compares the ARSSI value with T_h. If it is not satisfactory (ARSSI below T_h), the MN continues broadcasting DIS bursts periodically (with respect to the *Hand-off Timer*). Upon detecting a high quality link (ARSSI above T_h), the *Discovery Phase* stops and the MN resumes regular data communication (with the new preferred parent) —*Data Transmission Phase*.

6. mRPL in Detail

This section details the mRPL design. We first describe the additional timers that improve the efficiency and reliability of the hand-off process. The enhanced control message packets and the priority assignment of reply packets (DIO messages from neighbor APs) are then described. The Trickle timer setting (during the hand-off) and the parent selection are also discussed.

Timers. We have implemented four main timers to easily perceive the link degradation and the parent unreachability in a short period of time. The use of these timers within the *Data Transmission* and *Discovery Phase* is instantiated in Algorithms 1 and 2 and briefly described as follows.

(i) *Connectivity timer (T_C).* Mobile nodes constantly monitor the channel activity to detect any packet reception from their serving AP. Every MN runs a timer to increase the RPL routing responsiveness –The connectivity timer. The periodicity of the Connectivity timer is set according to the maximum Trickle interval (I_{max}). During this period, the MN keeps listening to the channel and monitors the incoming packets from the serving parent. Upon elapsing T_C, if the MN observes a silent parent, then it starts the *Discovery Phase*. Upon detecting any packet reception from the serving AP (e.g. Trickle DIO, unicast DIO or a data packet), Connectivity timer is reset.

(ii) *Mobility detection timer (T_{MD}).* Periodic DIS beaconing of the MN requests a unicast DIO message from the serving AP. The MN reads the ARSSI level related to the DIO message to assess the reliability of the link. Moving a node or appearing an obstacle between two nodes may result in losing the request or reply packets. In this situation, the MN starts the *Discovery Phase* to find a new serving parent. The periodicity of the Mobility detection timer is set according to the data generation rate at the MN.

(iii) *Hand-off timer (T_{HO}).* It is paramount to reduce the hand-off delay. This timer manages the periodicity of broadcasting bursts of DIS to the neighboring parents. This period should enable to accommodate transmitting bursts of DIS with the highest possible rate and receiving intermittent replies from neighbor nodes. The DIO replies are collected immediately after sending each burst. The sequence of sending replies by each parent is scheduled in such a way to reduce the probability of collision.

(iv) *Reply timer (T_R).* A serving parent is supposed to reply to the MN by unicasting a DIO control message at certain instants. Selecting a wrong moment to reply may cause a collision with the data packets, which in turn triggers the *Discovery Phase*. The parent node extracts relevant information from the packets that are received from the MN (e.g. data packet counter in each window size). The reply time is calculated by $(ws - C) \times T_{DIS}$, where C represents the counter of DIS packets within each window size (ws) and T_{DIS} indicates the DIS interval. This reply time is adaptively changing upon receiving

new packets.

Algorithm 1: *Data Transmission Phase*

```
begin
    if received DIO packet then
        reset T_C;
        if ARSSI < T_l then
            go to the Discovery Phase;
        else
            continue the Data TX Phase;
        end
    else if T_MD expires then
        reset T_MD;
        unicast burst of DIS;
        go to the begin;
    else if T_C expires then
        go to the Discovery Phase;
    end
end
```

Enhanced control messages. To integrate the smart-HOP algorithm within RPL, we enhanced the RPL control messages rather than creating new ones. This approach guarantees backward compatibility with the standard RPL, i.e. standard RPL nodes can coexist and inter-operate with smart-HOP-enabled nodes in the same network.

RPL control messages are transmitted on a regular basis; however, during the hand-off process, they follow specific rules. In the *Data Transmission Phase*, the DIS is sent from the MN to the AP (unicast) and the preferred parent replies with a unicast DIO. The type of DIS and DIO is detected by reading a flag that reflects the status of each node (will be explained next). In the *Discovery Phase*, the MN multicasts DIS messages to all neighboring APs and receives unicast DIO replies.

smart-HOP enables transmitting unicast DIS control messages to probe the serving AP in order to ensure the parent is reachable and reliable (RPL transmits multicast DIS and DIO packets). To distinguish between the mRPL DIS and the native RPL DIS, a one bit flag (*F-DIS*) is implemented —see Fig-

Algorithm 2: *Discovery Phase*

```
begin
    if received unicasted DIS message then
        store RSSI readings;
        store counter value C of the latest DIS packet;
        reset T_R with (ws − C) × T_DIS;
        if T_R expires then
            calculate average RSSI;
            send unicast DIO message with average RSSI;
        else
            continue Discovery Phase;
        end
    else
        continue the Data TX Phase;
    end
end
```

ure 4(a). Initializing this field to "0" represents the multicast transmission of the RPL DIS. Instead, setting this field to "1" reflects the unicast mRPL DIS transmission. The additional two bits of "C" describe the counter of DIS messages within a window size. In mRPL with $ws = 3$, the counter increments to a maximum of 3.

The mRPL DIO message adds two fields: (1) *F-DIO* that stands for the flags and (2) $ARSSI$ that holds the average RSSI reading at the potential parent node —see Figure 4(b). The two bits of *F-DIO* distinguish three cases: (i) *F-DIO*=0 corresponds to the RPL DIO, (ii) *F-DIO*=1 indicates the mRPL DIO within the *Data Transmission Phase*, and (iii) *F-DIO*=2 reflects the mRPL DIO within the *Discovery Phase*.

Priority assignment. In order to reduce the packet collision during the *Discovery Phase*, we prohibit some of the APs to reply to the MN; parents with $ARSSI < T_h$ are excluded from the possible parents set and do not reply. To do this, each parent assigns a priority according to the average RSSI readings, as shown in Table 2. The priority assignment schedules the DIO transmissions in different slots. Since low-power networks are likely to operate in the transitional region, it is more likely that different parents choose the same slot. A

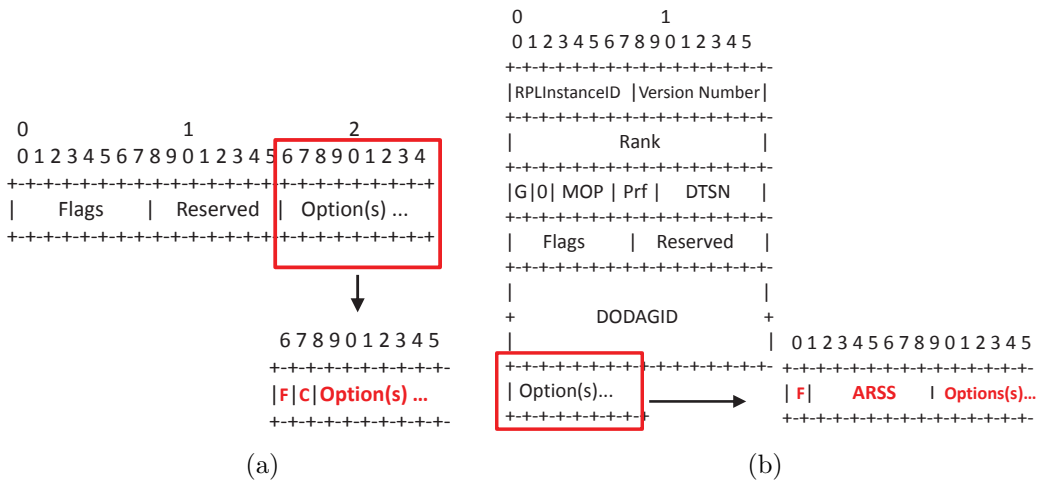

Figure 4: (a) The modified DIS packet format. Two fields of *F-DIS* and *C* are added to the RPL DIS packet, and (b) the modified DIO packet format. Two fields of *F-DIO* and ARSSI are added to the RPL DIO packet. Additional bits are applied to the "Option(s)" part of the packet.

Table 2: The priority assignment

Priority	Range of average RSSI readings
$prio = 1$	$-85 < ARSSI < -80$ dBm
$prio = 0$	$ARSSI \geq -80$ dBm

timer schedules the DIO transmission (t_{offset}) after detecting a busy channel as follows.

$$t_{offset} = (ws - C) \times T_{DIS} + t_2 \times prio + rand(t_1, t_2) \quad (1)$$

The first part of this equation, $(ws - C) \times T_{DIS}$, is the waiting time for receiving the complete DIS messages transmitted, which is similar to the *Data Transmission Phase* of the smart-HOP algorithm. We force the higher quality APs ($prio = 0$) to transmit earlier ($t_2 \times prio = 0$ ms) and the lower quality APs ($prio = 1$) transmit later ($t_2 \times prio = t_2$ ms). A random delay is also added to reduce the possibility of colliding the same priority level APs by $rand(t_1, t_2)$. It is important to note that with $t_2 \times prio$, lower quality links wait at most

for t_2 ms, $(max((prio = 0) \times t_2 + rand(t_1, t_2)) = t_2)$, which is measured by $(prio = 1) \times t_2 = t_2$ ms. The random value also reduces the possibility of collision between the replies from the lower quality and the higher quality APs. Random values are set to 10 and 15 ms, which are above the maximum possible transmission rate[4]. Considering $ws = 3$ and $T_{DIS} = 15$ ms, in the worst case (i.e. $rand(t_1, t_2) = 15$ ms) it takes at most 75 ms for the MN to get all replies from the neighboring APs. In our system model, we are considering a wise deplyment of APs in order to avoid very high or very low density of APs. Our tests provide minimal overlap between contiguous APs that would prevent the possibility of having multiple high quality APs in a region.

Trickle setting during mRPL. According to the Trickle algorithm, all nodes (roots/routers) broadcast messages (DIOs) to exchange information with the neighbor nodes. The transmission interval is bounded and enlarged upon network stability. When a node moves, it interferes with the network stability and hence the interval is set to its minimum value (I_{min}). We keep the Trickle interval unchanged during the hand-off process, while keeping the transmissions' schedules independent. As already mentioned, the F fields of the control messages (*F-DIS* and *F-DIO*) are added to distinguish between mRPL and RPL messages.

Loop avoidance mechanism. In RPL, when a node disconnects from its parent, the *rank* value sets to infinity. This enables the MN to connect to any neighboring node, even the ones with a lower *rank*. For instance, the MN may select a neighbor node that was previously the MN's child (before the hand-off) as the new parent. Since the neighbor has a lower *rank* compared with the infinity, according to the default RPL, the MN is allowed to choose

[4]We use Tmote Sky motes that are equipped with the Chipcon 2420 radio chip [42], operating at 2.4 GHz with 250 kbit/s data rate. The packet size depends on the data payload, which is added to the header and footer. Since RPL runs an IPv6 addressing strategy, we assume that the packet size is 127 bytes in the worst case. Considering the radio data rate and the packet size, the node is able to transmit at most 246 packets/s (1 packet every 4 ms). The propagation delay, modulation, demodulation, fragmentation and de-fragmentation extend this approximate transmission delay. In real world experiments, it is wise to pick intervals larger than 4 ms to ensure successful transmissions.

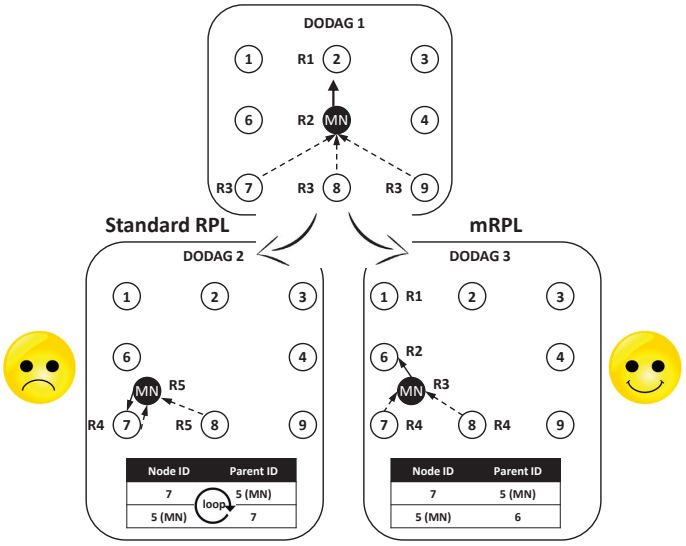

Figure 5: The DODAG 1 updates upon mobility. The DODAG 2 updates by applying the standard RPL algorithm, increasing in a closed loop. The DODAG 3 updates according to mRPL, avoiding the closed loop.

it. As shown in Figure 5, in DODAG 1, Node 5 has a parent (Node 2) and three children (Nodes 7, 8 and 9). Each node delivers data to a lower rank node (written besides each node). When Node 5 moves out from the range of Node 2, according to the RPL routing, DODAG 2 is established. In this case, first the MN's rank is set to infinity and then it picks a neighbor with the highest ARSSI level and the lower rank level (6). Thus, Node 7 (Node 5's previous child) is selected as the preferred parent. The data messages from Node 5 are forwarded to Node 7, and Node 7 forwards to Node 5 (its parent), which represents a closed loop.

RPL has some loop detection mechanisms; however, loops can not be fully avoided and thus may still occur. To fix this, RPL performs global repairs where the routing tree is reconstructed, updating the rank of all nodes in a DODAG. This behavior is not efficient as a MN will need to start the whole process of finding a new parent again, which is highly time and energy consuming.

In this context, we devised a simple yet efficient loop avoidance mechanism. We analyzed two different approaches to avoid the loop effect. First, the

Table 3: Memory usage in standard RPL versus mRPL

Implementation	ROM (bytes)	RAM (bytes)
RPL (MN)	40,202	7,660
RPL (AP)	40,336	7,606
mRPL (MN)	44,348	8,562
mRPL (AP)	44,022	8,512

MN gets replies from all neighboring APs and then ignores the messages from the previous children. Thus, after creating the set of alternative parents, the children are excluded from the set. Second, the children decline to reply the previous parent's request for joining. We select the latter approach as it leads to less communication processing and overhead during hand-off. DODAG 3 in Figure 5 shows a scenario where Node 5 disconnects from Node 2 and connects to Node 6, avoiding to choose one of its previous children.

Memory overhead. The memory overhead of the standard RPL against the mRPL is illustrated in Table 3. smart-HOP has been integrated with about 4 kB ROM and 1 kB RAM extra, representing just 10% of additional footprint.

7. Simulation analysis

We implemented and tested the protocol with a simulator that easily ports to the sensor hardware and provides the opportunity of analyzing different network conditions. Since low-power wireless links are very prone to external radio interference from other wireless technologies operating in the ISM band, simulators are usually unable to provide a very accurate radio interference model. Each indoor/outdoor environment exhibits specific link behaviors that are impossible to mimic in the simulated environment. mRPL has been designed to perform well in networks with full AP coverage and minimum overlap between neighboring APs. In simulation, we are able to establish an environment that provides these requirements, but in real experiments, links may overlap differently (more or less). We will compare simulation and experimental results in Section 8 to show the necessity of performing experimental tests in order to

Table 4: Description of the RPL scenarios

Scenarios	I_{min}	$I_{doubling}$	DIO_{min}	DIO_{max}
(12-8)	12	8	4.096 s	1048.576 s
(12-1)	12	1	4.096 s	8.192 s
(10-2)	10	2	1.024 s	4.096 s
(8-1)	8	1	0.256 s	0.512 s

enrich the radio propagation and interference models in simulation.

7.1. Simulation setup

In order to implement and evaluate mRPL, we opted for the Contiki 2.6.1 [43] operating system (OS), which supports the Cooja simulator. The main reasons for selecting Contiki are: (i) the availability of a RPL/6LoWPAN implementation that is reasonably mature and widely used, (ii) the ease of porting Cooja code to the hardware platforms, and (iii) the availability of a mobility plugin in Cooja [44], that enables to evaluate mRPL in a repeatable environment[5].

In this section, we compare mRPL with different settings of the standard RPL, considering different topologies. Then, we study the impact of other parameters on the mRPL performance. The major parameters that impact the RPL performance are I_{min} and $I_{doubling}$ in the Trickle algorithm. We considered four RPL scenarios by varying the tuple $< I_{min}, I_{doubling} >$ values, as defined in Table 4. The evaluation focuses on the impact that these Trickle parameters have on five network metrics:

Hand-off delay. It represents the average time required to perform the hand-off process with mRPL or the time spent to discover a new preferred parent in the standard RPL.

Total packet overhead. We identify all the non data packets (control messages) as network overhead. RPL uses ICMPv6 based control messages (DIS,

[5]By default, Cooja does not support mobility. Nevertheless, based on the fact that each deployed mote has its own location represented in a two-axis (x,y) system, a Cooja mobility plugin [44] was developed that is capable of loading specific mobility trace-files using the Interval Format.

DIO and DAO) for building and maintaining DODAGs. The mRPL utilizes these control messages to detect the mobility and perform the hand-off process.

Packet delivery ratio (PDR). It is defined as the number of successfully received packets at all APs over the total number of packets sent from MNs. The successful delivery rate of mRPL is compared with different RPL scenarios in the presence of mobility.

Network throughput. This metric shows how frequently data information flows across the channel or network [45]. It is defined as the total number of bits received per second. To calculate this metric, only data packets are taken into account, i.e. the control messages are excluded. In general, the aim of this metric is to show the maximum data rate that mRPL can cope with. In fact, we should consider that the data rate cannot exceed a boundary by considering the processing, propagation and communication delays. The idea behind choosing the maximum data rate is to evaluate the algorithm for scenarios with more demanding QoS requirements.

Total DAO packets. To establish downward routes, RPL nodes send unicast DAO message upward. The next hop destination of a DAO message is the preferred parent. After switching to the best parent, the child node informs the previous parent about its disconnection and the selected parent about its reachability. The total number of DAO packets is an indication for assessing the routing responsiveness and the number of hand-offs in a mobility-enabled network.

7.2. RPL vs. mRPL

To evaluate the proposed algorithm, we consider three network typologies: (1) with two APs, (2) with four APs deployed in a row, and (3) with eight APs deployed in two parallel rows. In the first deployment with two APs (Node 1 and Node 2, 10 m apart —see Figure 6(a)), the MN travels 15 times between AP_1 and AP_2 with a constant speed ($v = 2$ m/s) and transmission power of -25 dBm, while generating data with the rate of 30 pkt/s. Similarly, in the two other deployments (Figures 7(a) and 8(a)), the MN moves from one left corner

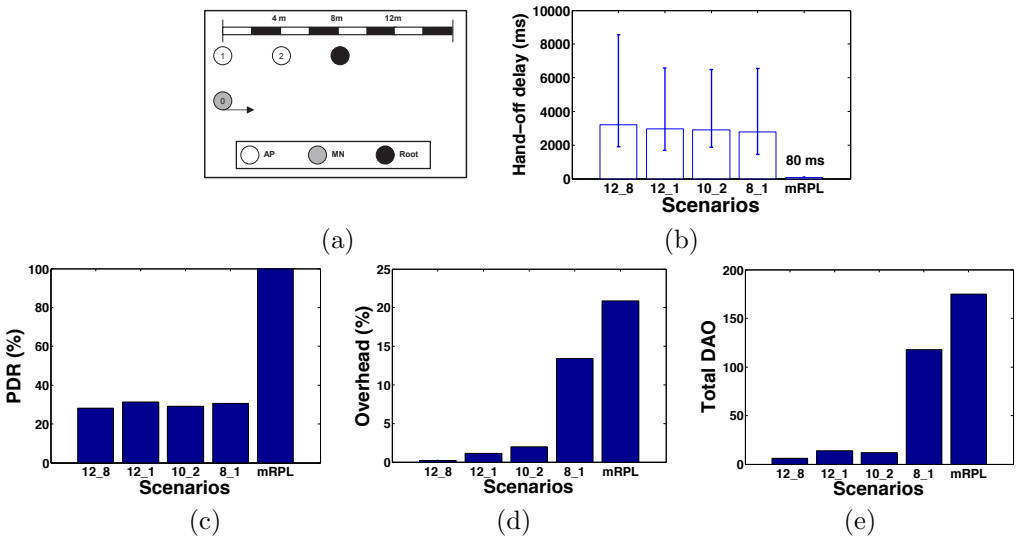

Figure 6: Simulation results for a network topology with two APs. (a) simulation scenario, (b) hand-off delay, (c) packet delivery ratio, (d) total overhead in terms of control messages, and (e) total number of DAOs.

to the right corner with the same constant speed and then returns back to the starting point.

Connectivity is guaranteed by providing a fast and reliable hand-off process. mRPL is able to detect and perform a hand-off within tens of milliseconds (80 to 83 ms), which is much faster than all RPL scenarios — see Figures 6(b), 7(b) and 8(b). We have estimated the hand-off delay in the standard RPL as it does not have a hand-off mechanism. The "hand-off" in RPL is assumed to start at the moment when packets start to get lost at the serving parent and to end when the new parent starts to successfully receiving data packets from the MN. The high data generation rate accelerates the updating of the ETX metric that leads to a fast parent switching process during link degradation.

The hand-off delay of RPL scenarios fluctuates a lot, as the mobility detection mechanism depends on various conditions (e.g. data rate, Trickle timer and ND protocol) and the responsiveness to environmental dynamics is not guaranteed in RPL. The average hand-off delay of RPL scenarios varies from 2776 ms

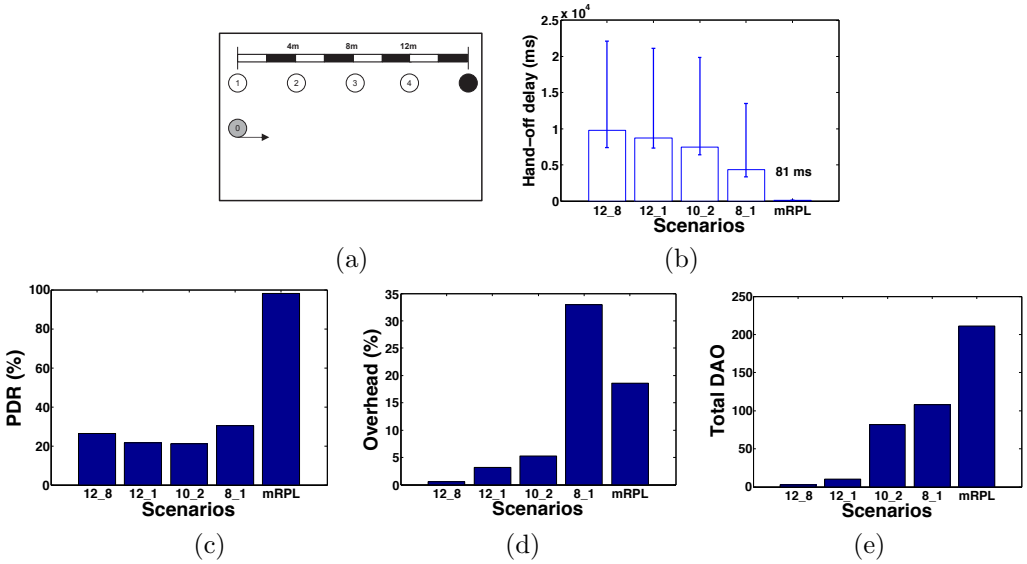

Figure 7: Simulation results for a network topology with four APs. (a) simulation scenario, (b) hand-off delay, (c) packet delivery ratio, (d) total overhead in terms of control messages, and (e) total number of DAOs.

to 9776 ms in these three network topologies (Figures 6, 7 and 8). In RPL, the mobile node switches between parent nodes in its parent set. In order to update the parent set information, it uses the Trickle and ND algorithms. The Trickle algorithm (that schedules the control message exchanges) will enlarge intervals in a stable network. To detect mobility in this condition, a RPL node either waits for receiving a NA message or requests this message by multicasting a NS message to its neighboring APs. These messages are supported by the ND protocol to detect parent unreachability. The major drawbacks of RPL concerning network connectivity are: (i) the sudden changes due to nodes mobility are not quickly detected if the network has been stable for a while, (ii) the ND protocol is initiated at the parent side (like a passive hand-off), which enlarges the hand-off duration, and (iii) resuming the ND protocol (that reconstructs the routing trees) is very expensive.

mRPL is able to provide near 100% packet delivery ratio. A fast hand-off process enables transmitting most of the packets to the targeting access point. In RPL, the MN should wait for control messages from the nearest AP.

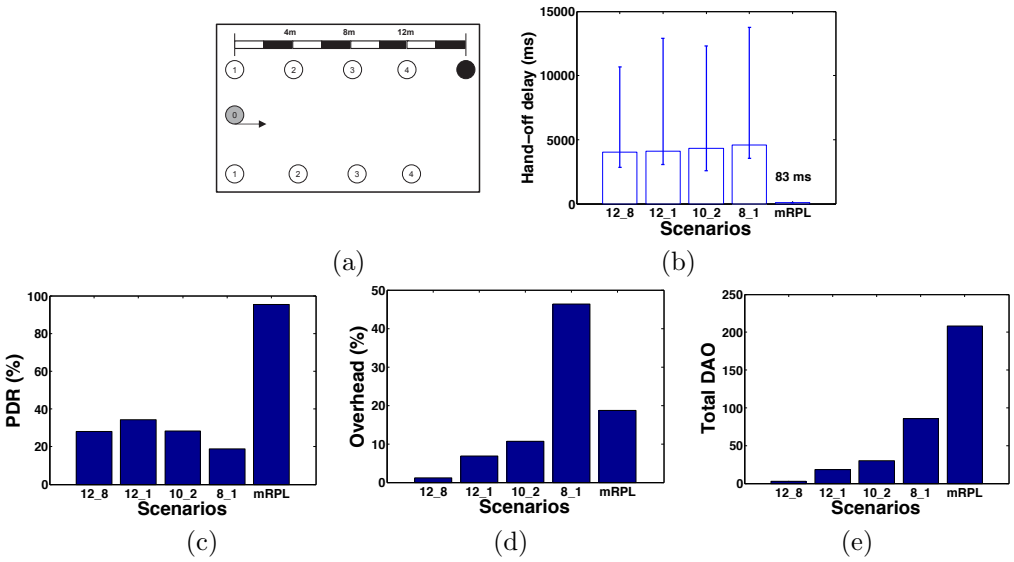

Figure 8: Simulation results for a network topology with eight APs. (a) simulation scenario, (b) hand-off delay, (c) packet delivery ratio, (d) total overhead in terms of control messages, and (e) total number of DAOs.

A longer delay causes more packet losses as the MN is not connected to any AP. In mRPL, the MN is able to send data to the previous parent during the *Discovery Phase* until finding a new preferred parent. This mechanism increases the chance of delivering most of the data packets, as shown in Figures 6(c), 7(c) and 8(c).

The control message overhead of mRPL is comparable with the RPL settings with maximum overhead. In RPL, after creating DODAGs during an initialization phase, if the network remains stable, the periodicity of control message exchanges will converge to its maximum value. For instance, according to Table 4, in the $< 12, 8 >$ RPL scenario, the periodicity is 1048.576 s and with $< 8, 1 >$ is 0.512 s. A higher message transmission rate increases the network overhead. In mRPL, the Trickle parameters are set according to the RPL scenario with lowest overhead ($< 12, 8 >$). The additional control messages triggered by the hand-off are invoked on-demand. Hence, in a high data rate network, similar to our example (with 30 pkts/sec), mRPL has a higher amount of overhead compared with RPL. Comparing different network topologies shows

that adding more neighbor nodes (APs) increases the overhead of the network — see Figures 6(d), 7(d) and 8(d). Adding more APs in the neighborhood of a MN would increase the number of reply packets in the *Discovery Phase*, eventually increasing the overhead.

mRPL is very responsive to network dynamics. The total number of DAOs is an indicator for showing the effort for creating new connections. Since RPL does not have an explicit hand-off mechanism, a successful parent selection is identified by DAO transmissions. In Topology 1 (with two APs), mRPL has the greatest number of new connections, which shows an accurate hand-off during each trip. Adding more APs in Topology 2 results in creating more connections in both RPL and mRPL. In a denser deployment (Topology 3), there are more overlaps between links and hence the total number of DAOs reduces in RPL and mRPL. However, mRPL is still able to smoothly switch between APs with only 1.4% less hand-offs, while RPL reduces new connections up to 63%.

7.3. Further evaluations on speed, duty cycling and network density

At this stage, we are aiming at studying the impact of mobile node speed and network duty cycling on the performance in high and low data traffic in a more complicated network deployment. We employ a MN and 12 APs located in four rank levels as depicted in Figure 9(a). MN starts its trip from the vicinity of AP_1 and travels all the network through the dotted lines, then pausing for 30 seconds at the initial position, while the simulation is run for two minutes.

mRPL is efficient for the range of normal human walk speeds. In our simulations, we applied speeds 0.5, 1, 2, 3 and 4 m/s to various network traffic scenarios. Considering each data transmission period, we observe that an increase in the MN speed does not affect the network performance as depicted in Figures 9(b), (c) and (d). Slight variations in the results with different speeds is mainly due to the changes in hand-off moments.

mRPL has less overhead in low traffic networks. In mRPL, mobility detection is according to the link degradation (ARSSI) and connectivity timer

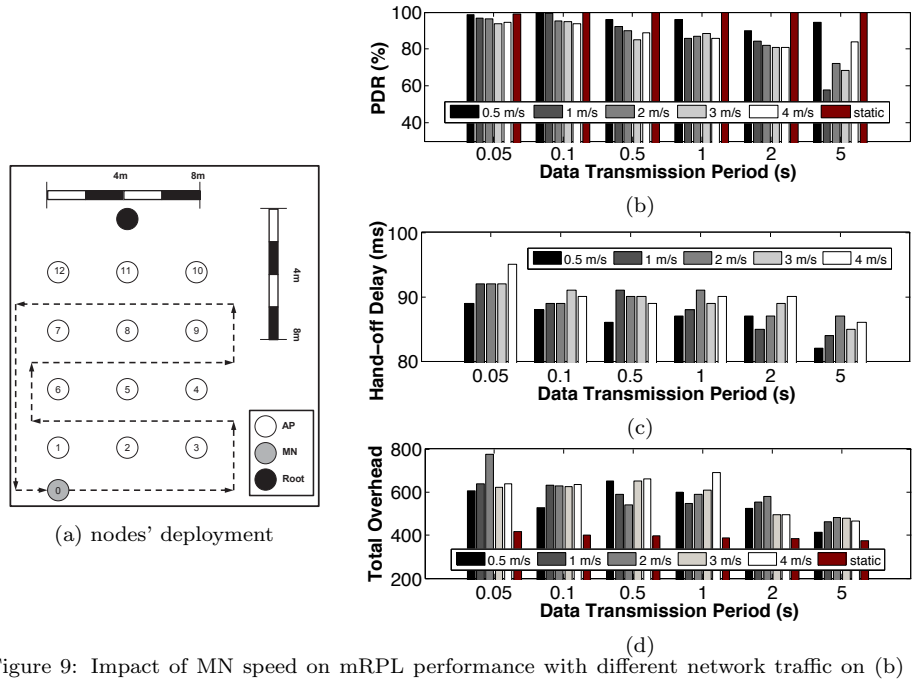

(a) nodes' deployment

(b)

(c)

(d)

Figure 9: Impact of MN speed on mRPL performance with different network traffic on (b) packet delivery ratio, (c) average hand-off delay, and (d) total overhead.

(T_c). We adapt the connectivity timer according to the data transmission interval to reduce the network overhead. A fixed and low interval connectivity timer in low traffic scenarios imposes high amount of overhead. For instance, the overhead in a low data traffic scenario (e.g. transmitting data every 5 s) is 30% less than the high data traffic scenario (e.g. transmitting data every 50 ms).

Low traffic scenarios require data retransmissions to keep network reliability. By enlarging the connectivity timer in low traffic scenarios, some of the data packets may drop. Upon data packet losses, hand-off process resumes that leads to parent switch. After the hand-off, MN has a good connectivity with the preferred parent. Therefore, we propose a data retransmission to the new AP immediately after the hand-off process to keep network reliability.

Hand-off delay is constant regardless of network traffic and mobile node speed. A hand-off in mRPL is a process that requires a number of packet exchanges to assess neighbor APs. This process is very fast and takes about 90 ms with some fluctuations in various scenarios.

We also evaluated mRPL without existence of mobile node. Figures 9(b) and

(d) show that **a static node is able to successfully transmit almost all data packets to the fixed infrastructure.** The overhead of this experiment is the minimum, since additional control messages are not generated in a static environment.

The duty cycling MAC design (ContikiMAC) reduces the energy consumption by periodic idle-listen periods. In ContikiMAC, if a packet transmission is detected during a wake-up period, the radio is kept on to receive the packet. After successfully receiving a packet, receiver sends a link layer acknowledgment. According to this behavior, in mRPL, MN keeps sending burst of DIS messages until receiving and replying by the neighbor AP as depicted in in Figure 10 (a). The radio of Receiver 1 is always on (NullMAC) and can immediately detect the packet transmissions from the MN, and thus, the hand-off process is the shortest possible. By applying a duty cycling approach, the request packets are detected later and the hand-off process takes longer (MN keeps sending burst of DIS messages until receiving a reply from a neighbor AP). Increasing the sleeping period worsens the performance in terms of responsiveness (compare Receiver 2 to Receiver 3)[6].

Increasing the listening period degrades the hand-off performance. We have analyzed the duty cycling approach by changing channel check rates (64, 32 and 8 Hz) and studied the network performance –see Figures 10 (b)-(d). Reducing the check rates increases the listening periods that enlarges the hand-off delay. By increasing the check rate from 64 Hz or 15.625 ms to 8 Hz or 125 ms (87.5% increase in listening period) with 1 (s) data transmission period, the hand-off delay increases from 115 ms to 156 ms (i.e. 26% increase), which is reasonable. Consequently, long hand-offs reduces the packet delivery ratio and increases the control message overhead. The trend of network performance degradation by increasing the listening period is similar in all scenarios with

[6]In ContikiMAC it is required to obey a precise timing between transmissions. It uses *Clear Channel Assessment* (CCA) that reads the RSSI measurement to detect channel activity. The timing analysis in [46] shows that a minimum packet size of 23 bytes is required for the CCA mechanism to work properly. We respect this limitation in our simulations and experiments as the size of IPv6-based packet are normally much longer.

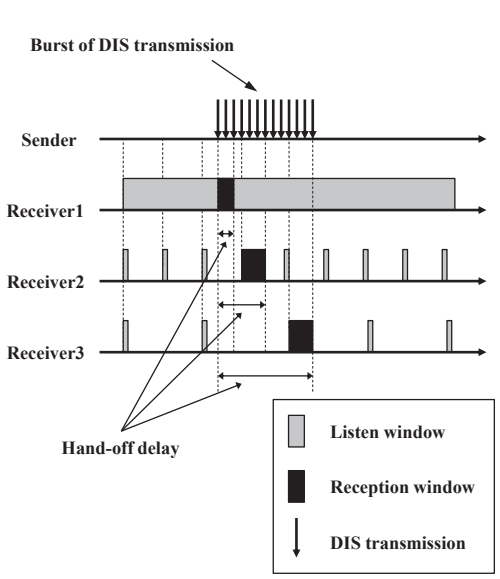

(a) Example of hand-off delay with different duty cycles.

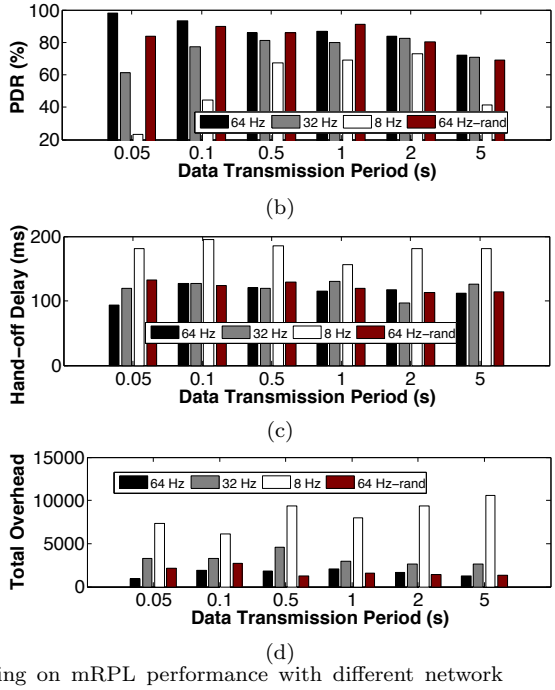

Figure 10: Impact of network duty cycling on mRPL performance with different network traffic on (b) packet delivery ratio, (c) average hand-off delay, and (d) total overhead.

various data transmission periods.

The mobility pattern does not affect the hand-off performance. From results in Figures 9, we learned that mobile node speed does not affect the performance. However, there are slight fluctuations in the results, which are imposed by changing the hand-off moments due to the reception of control messages sooner or later. We created a random mobility pattern, where speed, direction and pauses of mobile node randomly change. Figures 10 depicts the results of random mobility with 64 Hz duty cycle. In general, the delivery ratio, hand-off delay and the total amount of overhead is very similar to the constant speed scenario (2 m/s) with 64 Hz duty cycling.

Network density has a direct impact on the network overhead. Increasing the number of APs in a single broadcast domain increases the number of DIO replies in the *Discovery Phase* of a hand-off process, as depicted in Figure 11(b). This also increases the network overhead of mRPL. A wise deployment of APs in a real experiment reduces the network overhead drastically.

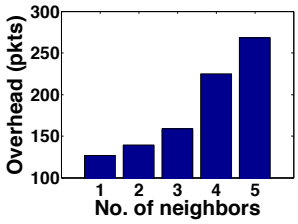

Figure 11: Impact of network density on total overhead.

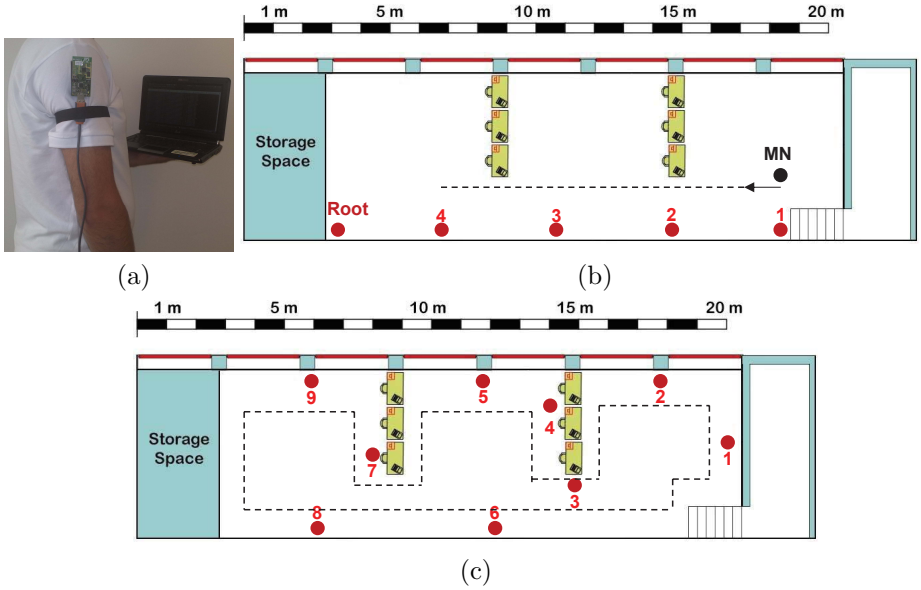

Figure 12: Experimental evaluation, (a) the MN attached to the shoulder, (b) Experimental Setup 1 with 4 APs and a MN deployed in a row, and (c) Experimental Setup 2 with 9 APs distributed across the lab.

8. Experimental Evaluation

In this section, we explain the experimental network setup in order to test and compare RPL and mRPL. The parameters setting, topological configuration and the scenarios are described.

8.1. Network Setup

In order to perform realistic experiments, we attached the mobile node to a person's body (Figure 12(a)) and connected to the logging PC[7] to collect the information. The experiments were held in big room with 80 m^2 size and all nodes were running with their minimum transmission power (-25 dBm).

Figure 12(b) (Setup 1) shows a scenario where contiguous APs provide minimal overlap. This situation was achieved by selecting the lowest transmission power (power level = 1) and locating APs with a 0.3 m separation.

In a more realistic scenario, Setup 2, we randomly deployed 9 APs in the room (as depicted in Figure 12(c)). The APs were attached to walls at 1.5 m height from the ground (to guarantee a better connectivity). We will show the results later in this section.

RPL configurations. In general, RPL devices play the role of a router or root node. In our experiments, we consider a single root that collects all data. The access points and the mobile nodes are routers; the MNs generate data and the APs forward them to the root.

In order to compare RPL with mRPL, we created the best possible RPL setting to switch fast between parents when a child moves. Typically, in RPL, a child node needs to detect a high ETX value to trigger a parent switch. The frequency of ETX updates depends on the network traffic in terms of rate of data/control exchanges. We considered the highest possible data rate to increase the RPL routing responsiveness to network dynamics.

8.2. Results and Discussion

Experimental Setup 1. We compare various RPL scenarios with mRPL in a simple network topology presented in Figure 12(b), which provides minimum overlap between contiguous APs. All nodes run NullMAC (full-time on), which

[7]At the beginning, we connected all APs to one laptop with passive USB cables and USB2.0 hubs. Then we observed some data loss during data transfer through the UART port. Adding more PCs did not solve the problem completely. Hence, we managed to get the data log from the MN with the cost of a person carrying a laptop during the experiment.

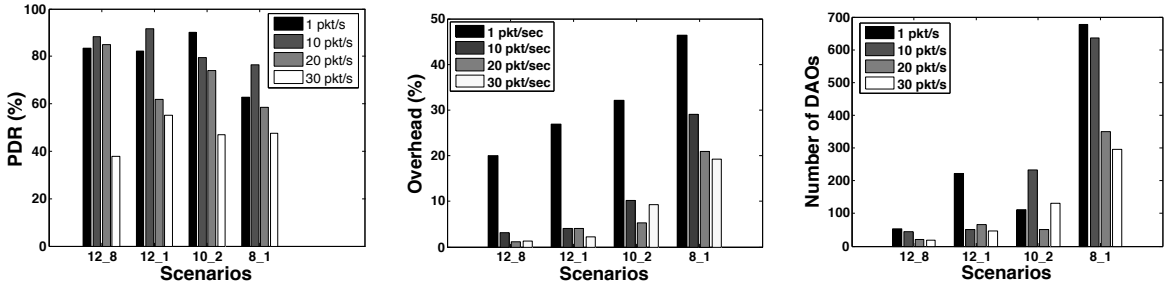

(a) (b) (c)

Figure 13: Experimental Setup 1, Comparing several RPL scenarios in terms of (a) packet delivery ratio, (b) overhead, and (c) number of DAOs.

is more useful for comparing mRPL and mRPL without the effect of packet losses and inherent delays in a duty cycling protocol.

First, we evaluate the packet delivery ratio of various RPL scenarios (previously defined in Table 4) with different data rates. Our analysis indicates that **higher traffic leads to lower packet delivery ratio.** Smaller values of the Trickle timer and a higher data generation rate increase the network traffic, which in turn increases the chance of packet collision —see Figure 13(a). The packet drops are more significant in larger Trickle timers (e.g. $< 12, 8 >$), which results in nearly 46% packet drops when increasing the data rate from 1 to 30 pkt/s, while the lowest timer setting ($< 8, 1 >$) exhibits nearly 29% drops.

Smaller values of the Trickle timer impose higher control packets overhead in RPL. The overhead is calculated according to the percentage of the ICMPv6 packets over the total number of packets (ICMPv6 packets + data packets). Figure 13(b) shows that the overhead of RPL increases when choosing smaller Trickle values ($< 8, 1 >$ results in more control message exchanges than in the other scenarios). A lower data transmission rate results in a higher percentage of control messages with respect to the total number of packet exchanges.

Successful parent switching is based on the data rate and the Trickle setting. The number of DAOs corresponds to the number of new links created between a child (MN) and a neighboring parent. A high data

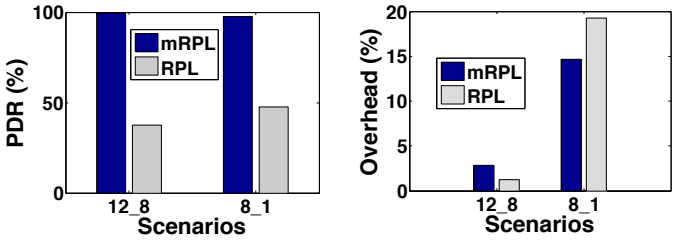

(a) (b)

Figure 14: Compare RPL and mRPL in terms of (a) PDR and (b) overhead in Experimental Setup 1.

transmission rate increases the ETX value updates. Figure 13(c) shows that in all settings, the higher the packet rate, the lower the DAO transmissions. Additionally, smaller Trickle values increase the number of DAO packets.

mRPL performance is independent of the Trickle setting. In fact, mRPL uses RPL control messages as a backup mechanism. We compared mRPL with two extreme RPL scenarios ($< 12, 8 >$ and $< 8, 1 >$). Figure 14(a) shows that regardless of the Trickle setting, mRPL copes with correctly delivering most of the data packets (nearly 100%). Note that reducing the Trickle timers decreases the mRPL packet reception rate by only 2%, as the data packets are more prone to collide with the control packets. The use of Trickle as a backup in mRPL raises the overhead of the algorithm in terms of additional control message exchanges. Hence, in mRPL it is recommended to use a low overhead Trickle setting (e.g. $< 12, 8 >$, as depicted in Figure 14(b)).

Experimental Setup 2. We extended the tests by deploying APs as depicted in Figure 12(b). All nodes were tuned to transmit power level 3 (-25 dBm), which created higher overlap between the neighbor APs. A root node was placed in the center of the room. The mobile node was attached to a person's arm (along the dashed path and it was generating packets at different rates.

A higher overlap of the wireless links increases the packet delivery ratio. Apparently, by creating more AP coverage overlapping, more packets have the possibility to reach the destination. However, RPL cannot support high transmission rates under mobility, as shown in Figure 15(a). Contrarily,

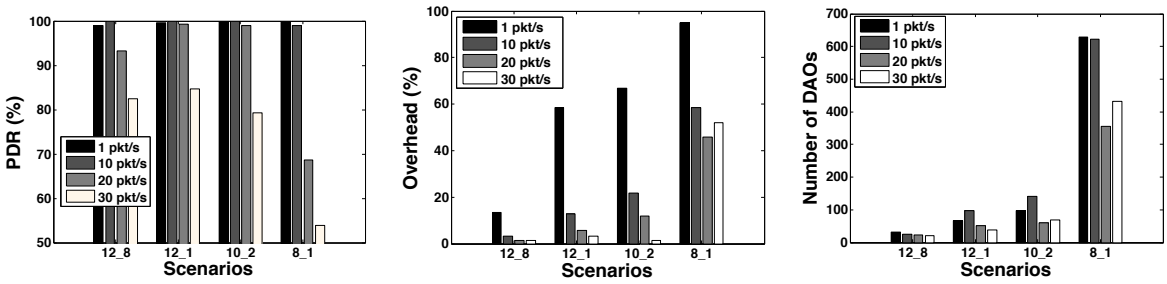

(a) (b) (c)

Figure 15: Experimental Setup 2, Comparing various RPL scenarios in a more realistic network topology in terms of (a) packet delivery ratio, (b) overhead, and (c) number of DAOs.

our experiments revealed that in an extreme condition with 30 pkt/sec data rate, mRPL still forwards 99.7% of data packets.

Figure 15(b) shows the overhead of RPL scenarios with different data rates. The trends are similar to the Experimental Setup 1. The best RPL setting with high data rate is $< 12, 8 >$, which leads to the lowest overhead. To update the routing information, RPL benefits from the data as well as control message exchanges. With the same setting in a high data rate application (30 pkt/s), mRPL resulted in 1% additional control messages overhead.

Higher links overlaping reduces the possibility of parent switching. The number of new links is smaller than for experimental Setup 1. By comparing the results in Figure 13(c) and Figure 15(c) in a high data rate condition, we conclude that the new links establishment (in a more realistic network topology) for $< 12, 8 >$ and $< 8, 1 >$ RPL scenarios reduces by 14% and 31%, respectively. Thus, we infer that higher links connectivity postpones the process of parent switching, and hence decreases the number of DAOs.

Standard RPL has no built-in hand-off mechanism. Therefore, it is hard to calculate the hand-off delay in RPL. In simulation, we have presented a rough estimation of the hand-off delay for different RPL scenarios. Empirical results show that mRPL has a very fast parent switching process with about 88 ms hand-off delay, leading to a very high packet delivery ratio even with high data transmission rates.

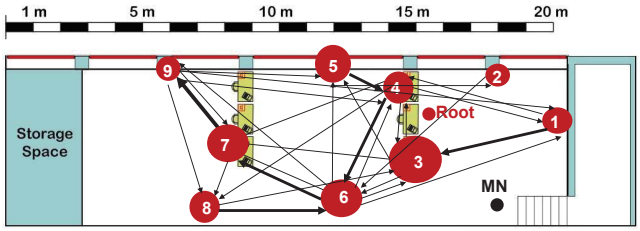

Figure 16: Mobile node movement representation in Experimental Setup 2.

Further insight into Experimental Setup 2. Indoor experiments impose some limitations on the overall performance. The location of APs, furniture, people and the external interference affect the hand-off performance. In Figure 16, the arrows correspond to the parent switching (from one AP to another). The thickness of the arrows indicates the amount of hand-off/s in the correspondent link. Note that hand-offs are not always performed between the closest APs. This means that the high variability of low-power wireless links and the dynamic behavior of the mobile network may dictate not choosing the closest APs. Figure 16 also illustrates (with circles) the amount of packet exchanges with mRPL at each AP. Larger circles means more packets received (Nodes 3, 5, 6 and 7). Nodes in a good connectivity region (central location) can maintain the connection longer than the ones on the right and left sides of the room (Nodes 1, 2, 8 and 9); hence more packets are successfully received by "central" APs.

Figure 17 shows the packet delivery ratio and the average RSSI at each AP (links 1 to 9 from the MN to the APs). There is a correlation between the average RSSI and the PDR in each link (higher ARSSI leads to higher PDR). This means that a hand-off triggered within the transitional region of the wireless link can result in a very good performance. Keeping the average RSSI and the PDR high requires a very careful decision on the moments of starting and ending a hand-off: closer to the lower threshold of the transitional region would reduce the packet delivery drastically. Nodes 3 and 7 are more benefited as they are placed in more strategic places with better ARSSI.

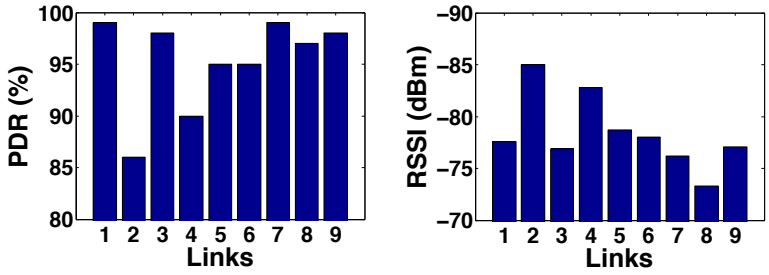

Figure 17: Packet delivery ratio and the average RSSI measurement of each link in Experimental Setup 2.

Table 5: mRPL: simulation versus experimental results

Scenarios	Sim. results	Exp. results
Setup 1 (Figure 12(b))	PDR=98.12% Overhead=18.8% Delay=81 ms	PDR=99.77% Overhead=7.63% Delay=92.7 ms
Setup 2(Figure 12(c))	PDR=99.56% Overhead=2.85% Delay= 86.21 ms	PDR=99.68% Overhead=2.43% Delay= 88.2 ms

8.3. Simulation vs. experimental results

We compared the results of the simulation with the experimental tests in the two network setups: (i) Experimental Setup 1 as depicted in Figure 12(b) and (ii) Experimental Setup 2 as depicted in Figure 12(c)). The results in Table 5 show that the performance in terms of packet delivery and hand-off delay in the experimental tests are relatively better than the simulation. The overhead in Setup 2 reduces drastically as the link overlap between the neighbor APs is higher than in the simulation. Moreover, the radio model of the simulator is inaccurate (mainly based on the distance between the nodes). However, in the real world, various physical and environmental parameters affect the radio model.

9. Conclusion

This paper proposes a very simple yet effective solution to cope with mobility as one of the challenging issues for future IoT applications. We extend

RPL —the standard routing protocol for the low-power networks in the IoT architecture— with fast and reliable mobility support.

We smoothly integrated a hand-off mechanism (dubbed smart-HOP) within RPL in a way to keep backward compatibility with the standard protocol. The smart-HOP hand-off mechanism [17, 18] was applied to mobile nodes (MNs) by managing the schedules of the control messages within the Trickle algorithm (DIS, DIO and DAO). A MN selects a new preferred parent according to the average RSSI (ARSSI). Neighboring nodes within the child set of the MN are ignored, to prevent routing loops.

We implemented some timers to increase hand-off efficiency by reducing hand-off delays and network congestion. We considered the low-power link characteristics and the limitations of the IPv6 architecture to tune the schedules. We applied priorities to APs (according to the ARSSI levels) to minimize the probability of packet collisions during the hand-off process.

The integration of smart-HOP within RPL (dubbed mRPL) was tested, fine-tuned and validated through extensive simulations and experiments. The results we obtained indicate that an inaccurate radio propagation model in the simulator impacts results related to the hand-off performance: radio links overlap more significant in real experiments (the simulator creates a minimum overlap between neighbor APs).

We also found that the best setting of RPL parameters for mobile applications leads to a huge control message exchange overhead. Instead, mRPL is able to keep a low overhead while being responsive to network changes ($\approx$ 90 ms hand-off delay). Moreover, nearly 100% packet delivery rate is achieved upon mobility.

We studied the impact of varying network traffic, duty-cycling and mobile node speed on the mRPL hand-off performance. The results indicated that in low traffic networks, the hand-off process is less responsive. Moreover, enlarging the listening periods affects the performance by increasing the hand-off delay. However, the variation of mobile nodes speed (within the range of human walking speed) does not affect the overall performance.

We implemented and integrated our hand-off mechanism in the RPL/6LoWPAN stack in Contiki, a widespread operating system for low-power wireless networks. Importantly, we made the source code freely available to the international community [1].

Acknowledgments

This work was partially supported by National Funds through FCT (Portuguese Foundation for Science and Technology) and by ERDF (European Regional Development Fund) through COMPETE (Operational Programme 'Thematic Factors of Competitiveness'), within projects FCOMP-01-0124-FEDER-037281 (CISTER), FCOMP-01-0124-FEDER-014922 (MASQOTS).

References

[1] mrpl: smart-hop within rpl (2014).
URL `http://www.cister.isep.ipp.pt/masqots/sources.html`

[2] G. Mulligan, The 6lowpan architecture, in: Proceedings of the 4th workshop on Embedded networked sensors, ACM, 2007.

[3] G. Montenegro, N. Kushalnagar, J. Hui, D. Culler, Transmission of ipv6 packets over ieee 802.15. 4 networks, Internet proposed standard RFC 4944.

[4] T. Winter, Rpl: Ipv6 routing protocol for low-power and lossy networks (2012).

[5] Final report from the nsf workshop on future directions in wireless networking (November 2014).
URL `http://ecedha.org/docs/nsf-nets/final-report.pdf?sfvrsn=0`

[6] European commission, "factories of the future 2020: multi-annual roadmap for the contractual ppp under horizon 2020", research roadmap produced by the european factories of the future research association (effra) (2014).

URL http://www.effra.eu/attachments/article/129/Factories%20of%20the%20Future%202020%20Roadmap.pdf

[7] P. J. Marron, D. Minder, S. Karnouskos, The Emerging Domain of Cooperating Objects, Springer, 2012.

[8] J. Caldeira, J. Rodrigues, P. Lorenz, Toward ubiquitous mobility solutions for body sensor networks on healthcare, IEEE Communications Magazine, 2012, 50 (5).

[9] Smartfactory—towards a factory-of-things, Annual Reviews in Control, 2010, 34 (1).

[10] G. Wu, S. Talwar, K. Johnsson, N. Himayat, K. Johnson, M2m: From mobile to embedded internet, IEEE Communications Magazine, 2011, 49 (4).

[11] Ginseng: performance control in wireless sensor networks (2014).
URL http://www.ucc.ie/en/misl/research/previous/ginseng/

[12] Fasys: Absolutely safe and healthy factory (2014).
URL http://www.fasys.es/en/proyecto.php

[13] flexware : Flexible wireless automation in real-time environments (2014).
URL http://www.flexware.at/

[14] J. Martinez-de Dios, A. Jimenez-Gonzalez, A. San Bernabe, A. Ollero, Conet integrated testbed architecture, in: A Remote Integrated Testbed for Cooperating Objects, SpringerBriefs in Electrical and Computer Engineering, Springer International Publishing, 2014, pp. 23–39. This work has been carried out within the Cooperating Objects European Network of Excellence http://www.cooperating–objects.eu/.

[15] O. Chipara, W. G. Griswold, A. N. Plymoth, R. Huang, F. Liu, P. Johansson, R. Rao, T. Chan, C. Buono, Wiisard: A measurement study of network properties and protocol reliability during an emergency response, in: MobiSys, ACM, 2012.

[16] R. Silva, J. S. Silva, F. Boavida, A proposal for proxy-based mobility in wsns, Elsevier Journal of Computer Communications, 2012, 35 (10).

[17] H. Fotouhi, M. Zuniga, M. Alves, A. Koubaa, P. Marrón, Smart-hop: A reliable handoff mechanism for mobile wireless sensor networks, in: EWSN, 2012.

[18] H. Fotouhi, M. Alves, M. Zuniga, A. Koubaa, Reliable and fast hand-offs in low-power wireless networks, IEEE Transactions on Mobile Computing, 2014.

[19] Z. Shelby, S. Chakrabarti, E. Nordmark, Neighbor discovery optimization for low power and lossy networks (6lowpan), Work in progress, IETF draft-ietf-6lowpan-nd-18.

[20] S. Cho, E. Jang, J. Cioffi, Handover in multihop cellular networks, IEEE Communications Magazine, 2009, 47 (7).

[21] I. Ramani, S. Savage, Syncscan: practical fast handoff for 802.11 infrastructure networks, in: INFOCOM, 2005.

[22] A. Mishra, M. Shin, W. Arbaugh, An empirical analysis of the ieee 802.11 mac layer handoff process, SIGCOMM 2003.

[23] M. Shin, A. Mishra, W. A. Arbaugh, Improving the latency of 802.11 hand-offs using neighbor graphs, MobiSys, 2004.

[24] C. E. Perkins, E. M. Royer, Ad-hoc on-demand distance vector routing, in: IEEE Workshop on Mobile Computing Systems and Applications, 1999.

[25] D. B. Johnson, D. A. Maltz, J. Broch, et al., Dsr: The dynamic source routing protocol for multi-hop wireless ad hoc networks, Ad hoc networking, 2001, 5.

[26] M. Pióro, Á. Szentesi, J. Harmatos, A. Jüttner, P. Gajowniczek, S. Kozdrowski, On open shortest path first related network optimisation problems, Performance Evaluation, 2002, 48 (1).

[27] A. H. Chowdhury, M. Ikram, H.-S. Cha, H. Redwan, S. M. S. Shams, K.-H. Kim, S.-W. Yoo, Route-over vs mesh-under routing in 6lowpan, in: Proceedings of the 2009 International Conference on Wireless Communications and Mobile Computing: Connecting the World Wirelessly, IWCMC '09, ACM, 2009, pp. 1208–1212.

[28] J. Vasseur, N. Agarwal, J. Hui, Z. Shelby, P. Bertrand, C. Chauvenet, Rpl: The ip routing protocol designed for low power and lossy networks, Internet Protocol for Smart Objects (IPSO) Alliance.

[29] J. Montavont, D. Roth, T. Noël, Mobile ipv6 in internet of things: Analysis, experimentations and optimizations, Ad Hoc Netw. 14 (2014) 15–25.

[30] D. Roth, J. Montavont, T. Noel, Performance evaluation of mobile ipv6 over 6lowpan, in: Proceedings of the 9th ACM Symposium on Performance Evaluation of Wireless Ad Hoc, Sensor, and Ubiquitous Networks, PE-WASUN '12, ACM, 2012, pp. 77–84.

[31] T. Narten, W. A. Simpson, E. Nordmark, H. Soliman, Neighbor discovery for ip version 6 (ipv6), RFC 2461, December 1998.

[32] G. Bag, M. T. Raza, K.-H. Kim, S.-W. Yoo, Lowmob: intra-pan mobility support schemes for 6lowpan, Sensors 9 (7) (2009) 5844–5877.

[33] K. Lee, R. Sudhaakar, L. Dai, S. Addepalli, M. Gerla, Rpl under mobility, in: Consumer Communications and Networking Conference (CCNC), 2012 IEEE, 2012, pp. 300–304.

[34] K. C. Lee, R. Sudhaakar, J. Ning, L. Dai, S. Addepalli, J. Vasseur, M. Gerla, A comprehensive evaluation of rpl under mobility, International Journal of Vehicular Technology 2012.

[35] I. Korbi, M. Ben Brahim, C. Adjih, L. Saidane, Mobility enhanced rpl for wireless sensor networks, in: Network of the Future (NOF), 2012 Third International Conference on the, 2012, pp. 1–8.

[36] J. Ko, M. Chang, Momoro: Providing mobility support for low-power wireless applications, Systems Journal, IEEE PP (99) (2014) 1–10.

[37] T. Watteyne, A. Molinaro, M. G. Richichi, M. Dohler, From manet to ietf roll standardization: A paradigm shift in wsn routing protocols, IEEE Communications Surveys & Tutorials, 2011, 13 (4).

[38] A. Woo, T. Tong, D. Culler, Taming the underlying challenges of reliable multihop routing in sensor networks, in: ACM SenSys, 2003.

[39] P. A. Levis, N. Patel, D. Culler, S. Shenker, Trickle: A self regulating algorithm for code propagation and maintenance in wireless sensor networks, 2004, in: NSDI.

[40] M. Zuniga, B. Krishnamachari, Analyzing the transitional region in low power wireless links, in: IEEE SECON, 2004.

[41] M. Z. Zamalloa, B. Krishnamachari, An analysis of unreliability and asymmetry in low-power wireless links, ACM TOSN 3 (2).

[42] T. Instruments, Cc2420 datasheet (2007).

[43] A. Dunkels, B. Gronvall, T. Voigt, Contiki-a lightweight and flexible operating system for tiny networked sensors, in: IEEE LCN, 2004.

[44] Mobility cooja plugin (2014).
URL `https://github.com/contiki-os/contiki/wiki`

[45] Q. Yan, M. Li, Z. Yang, W. Lou, H. Zhai, Throughput analysis of cooperative mobile content distribution in vehicular network using symbol level network coding, IEEE Journal on Selected Areas in Communications, 2012, 30 (2).

[46] A. Dunkels, The contikimac radio duty cycling protocol, SICS Technical Report, 2011.